metals

MDPI

Article

Elastic Thermal Deformation of an Infinite Copper Material Due to Cyclic Heat Supply Using Higher-Order Nonlocal Thermal Modeling

Ahmed E. Abouelregal [1,2] and Hamid M. Sedighi [3,4,*]

[1] Department of Mathematics, College of Science and Arts, Jouf University, Al-Qurayyat 75911, Saudi Arabia
[2] Department of Mathematics, Faculty of Science, Mansoura University, Mansoura 35516, Egypt
[3] Mechanical Engineering Department, Faculty of Engineering, Shahid Chamran University of Ahvaz, Ahvaz 61357-43337, Iran
[4] Drilling Center of Excellence and Research Center, Shahid Chamran University of Ahvaz, Ahvaz 61357-43337, Iran
* Correspondence: h.msedighi@scu.ac.ir or hmsedighi@gmail.com; Tel.: +9861-33226614-5768

Abstract: Thermoelastic modeling at nanoscale is becoming more important as devices shrink and heat sources are more widely used in modern industries, such as nanoelectromechanical systems. However, the conventional thermoelastic theories are no longer applicable in high-temperature settings. This study provides an insight into the thermomechanical features of a nonlocal viscous half-space exposed to a cyclic heat source. Using a novel concept of fractional derivatives, introduced by Atangana and Baleanu, it is assumed that the viscoelastic properties follow the fractional Kelvin–Voigt model. The nonlocal differential form of Eringen's nonlocal theory is employed to consider the impact of small-scale behavior. It is also proposed that the rule of dual-phase thermal conductivity can be generalized to thermoelastic materials to include the higher-order time derivatives. The numerical results for the examined physical variables are presented using the Laplace transform technique. Furthermore, several numerical analyses are performed in-depth, focusing on the effects of nonlocality, structural viscoelastic indicator, fractional order, higher-order and phase-lag parameters on the behavior of the nanoscale half-space. According to the presented findings, it appears that the higher-order terms have a major impact on reactions and may work to mitigate the impact of thermal diffusion. Furthermore, these terms provide a novel approach to categorize the materials based on their thermal conductivities.

Keywords: nonlocal thermoelasticity; higher-order time-derivatives; viscoelasticity; half-space medium; Atangana and Baleanu

Citation: Abouelregal, A.E.; Sedighi, H.M. Elastic Thermal Deformation of an Infinite Copper Material Due to Cyclic Heat Supply Using Higher-Order Nonlocal Thermal Modeling. *Metals* **2022**, *12*, 1927. https://doi.org/10.3390/met12111927

Academic Editor: Jiri Svoboda

Received: 16 September 2022
Accepted: 8 November 2022
Published: 10 November 2022

1. Introduction

Micro and nanoelectromechanical systems (M/NEMS) have great potential and are used in modern and highly sensitive microdevices across various industries. Due to their small size and different properties, these systems are used for mass detection, frequency synthesis, bioenergy, and light detection. Such mechanical systems are very sensitive, frequently consume low energy, and occupy a very tiny space [1]. By combining electrical and mechanical components, microelectromechanical systems (MEMS) have a typical length greater than one micrometer [2]. Their characteristic lengths govern the size-dependent mechanical behavior of nanomaterials and should be taken into account in structural designs. Micro-and nanomaterials with small dimensions often have different mechanical, electrical and thermal properties compared to macro-scale structures. Therefore, nano-scale devices such as nanowires, nanoplates and nanobeams are important candidates for studying the effects of size-dependency on the thermomechanical properties of such materials at sub-micron scales and their peculiar responses, quality factors, nonlinear damping and changes in Young's modulus may appear due to these superior characteristics [3–5].

The conventional elastic models studying the structural systems assume, as a basic principle, that the stress at any point can be entirely determined by considering the strain at that particular point and does not depend on the other components of strain tensor. According to recent experimental results on miniaturized structures, the traditional view of elastic behavior of materials, in which Young's modulus is constant regardless of their size and shape (according to Hooke's Law), has been challenged. Therefore, some modified models and hypotheses have been proposed to consider the observed phenomena in experiments by considering additional size-dependent and small-scale factors [6]. Small-scale effects in governing equations are usually ignored and less concerned in the classical continuum mechanics. To this end, several concepts and models, such as nonlocal elasticity, stress gradient theory, nonlocal stress gradient models, modified coupled stress theory, and stress-driven elasticity have been widely used to explain the small-scale effects [7–11]. Atomic lattice theory is related to the gradient concept in which the nonlocal elasticity and the small polar theory are combined to form the small-scale properties. Nonlocal elasticity explain the subtle structural properties of materials using a probabilistic mean of the attenuation function [12]. In recent years, the theory of nonlocal elasticity of all kinds has become a hot topic for scientists. The basic principle of nonlocal models is that the range of effects due to interactions between different material points is much wider than those of macro-scale materials.

In some particular situations, such as when the typical dimension of the structure is close to the internal characteristic length, the generalized thermoelasticity may be called into question. The mechanical and thermal characteristics of nanomaterials can be accurately predicted with the help of the molecular dynamic approach, but only for nanosystems with a finite number of molecules and atoms and of course with a lot of computational work. In contrast to the local models, nonlocal theories consider the fundamental equilibrium laws at the system's level [13]. Eringen [14–17] developed a nonlocal elastic model to address the local structural issues. He showed that the stress at any point in the medium may be regarded a function of the entire strain tensor everywhere in the body. This is because of the way that the nonlocal interactions work. The nonlocal theory contains the long-range interactions between points in a continuum material, which has significant ramifications for practical application. In a solid medium, charged atoms or molecules interact with one another over vast distances. The most popular theories that take into account the size-dependent behavior of structures are: strain gradient theory [18], nonlocal strain gradient elasticity [19], modified couple stress theory [20] and Silling's peridynamic model [21]. In recent years, new size-dependent models are developed with the help of fractional calculus theories. To address the difficulty of solving fractional partial differential equations (PDEs) and for time-dependent PDEs, Nawaz et al. [22,23] suggested a third-order explicit-implicit fractional system.

Numerous contributions have been made in recent years to investigate the response of micro- and nano-sized structure such as bars, wires, plates and beams in therapeutic applications based on the nonlocal concepts. There are also outstanding works applied on the problems of such systems to understand the behavior of cotemporary small devices such as energy harvesters, the mechanism of cancer spread in medicine, blood parasite detectors, resonators and accelerometers. To detect their sophisticated characteristics, numerical and experimental simulations were conducted on static, dynamic, and stability behavior of micro-/nanostructures, demonstrating the necessity of studying different models and methods applied to structural systems with small-scale dimensions [24–34].

Despite the fact that Duhamel and Neumann created the groundwork for the theory of thermoelasticity in the first half of the nineteenth century, widespread interests in this topic did not emerge until the years after the World War II. The reasons for this rapid and ongoing resurgence of interest are sound. When it comes to aeronautics, it has been discovered that the high speeds at which contemporary aircraft travels, causes the aerodynamic heating, which in turn causes the significant thermal stresses and, by reducing the elastic limit, diminishes the strength of the aircraft structure. In addition, the extremely high

temperatures as well as temperature changes in nuclear reactors affect their design and operation processes in the nuclear fields. Similarly, from engineering point of view, in the contemporary propulsion mechanisms such as rocket engines and jets, high temperatures in the combustion systems can produce undesired thermal strains. Spacecraft and missile technology, the physics of massive steam turbines, and even shipbuilding all experience similar phenomena where micro-cracks commonly being blamed on very mild thermal stresses. Countless theoretical and experimental studies detailing various elements of thermal stresses in engineering structures have resulted from dealing with the mentioned issues. Moreover, recently, linear viscoelasticity has become a mature science to explore the thermomechanical behavior of polymers, composites, solid propellants and materials that work well at high temperatures. Extreme temperature changes may cause physical failure in many parts of machines, especially those responsible for thermal protection in the aviation industry and other sectors where temperatures are usually high. In order to ensure the longevity, safety, and reliability of these parts, evaluations of the heat transfer and internal heat stress distributions are necessary. Microcracks can also form inside these machines, particularly during the production process when subjected to thermal or mechanical loading, which leads to a localized concentration of thermal stresses and temperature gradients.

There is no longer need to rely on the seemingly contradictory assumption made by classical thermoelasticity, which states that heat waves may travel through materials with unlimited rates; instead, this assumption has been broadened and refined. Tzou [35–37] substituted two distinct translations of the heat flux and the temperature gradient vectors for the basic Fourier's law. He presented the dual-phase-lag model to explain the temperature lag caused by phonon-electron interactions at the microscopic level and looked at how the solid body behaves in this situation. Abouelregal [38] used the fractional calculus and Taylor series expansion of time-fractional order to create a modified model of generalized thermoelasticity with multiple relaxation durations. In addition, he proposed a new thermoelastic heat conduction theory that takes into account two phase delays, together with the higher-order derivatives. In another work [39], he presented a refined model of heat conduction that incorporated a higher degree of a time derivative, thereby expanding Green and Naghdi's idea of heat conduction without energy loss.

In viscoelastic materials, the material response is determined by all previous stress states in addition to the current stress level. Fractional calculus, a field of mathematics, has recently been acknowledged as a useful tool to modify the viscoelastic theories. In the current work, by combining the fractional derivative of the Kelvin–Voigt viscoelastic model with the nonlocal theory, a new mathematical framework is proposed to investigate the thermoelastic behavior of a half-space medium. Furthermore, a modified type of heat equation is presented that incorporates the higher-order time derivatives and two-phase delays to describe the nonlocal thermoelasticity theory. In order to take into consideration the impact of fractional orders, the concept of Caputo and Fabrizio's fractional derivatives [40], which includes non-singular kernels, is applied. The nonlocal elasticity theory is then used to conduct a transient study of nanoscale half-spaces by considering the small-size effects. Although, the thermal wave model provides a macroscopic explanation for many crystals, the proposed thermoelastic model considers the most significant microstructural impacts which needs finite time to attain the local thermodynamic balance.

Numerous production processes involving metal cutting, spot welding, laser cutting/surface treatment, in addition to tribological purposes, such as ball bearing and gear designs, operate in the presence of stationary and variable heat sources. The metallurgical structural properties, thermal shrinkage, thermal cracking, hardness variation, residual stresses, and heat-impacted zones can all be altered by high-level temperature variations and rate of cooling close to the surface. In tribological applications, where the friction generates heat, understanding the temperature distribution is crucial for preventing thermal-related issues such as lubricant breakdown. Many electronic devices and systems rely heavily on the design consideration of thermal diffusion caused by variable heat sources and magnetic fields. These systems are often used in modern applications,

including, but not limited to, electronics, aircraft structural joints, surface thermocouples, boundary lubrication, nuclear reactors, biomedical devices, and ultra-hot liquid storage.

The introduced model will shed light on how the thermal waves propagate in a semi-infinite material when the features of size-dependent models are also considered. The medium is heated by an external source that varies in intensity over time and is immersed in a magnetic field. The Laplace transform method is used to obtain the numerical results for the physical variables. In-depth theoretical studies are also conducted to determine how the nonlocality of the stress field, viscoelastic factors, fractional order, higher-order constants, and phase lags affect the thermomechanical behaviour of a nanoscale half-space.

2. Nonlocal Fractional Thermoviscoelastic Model

In 1822, Fourier developed an empirical-based law describing the relationship between the heat flow and the magnitude of internal temperature gradient. Fourier's law may apply on the conventional Spatio–temporal problems, as follows [41]:

$$q_i(\vec{P},\tau) = -K\Theta_{,i}(\vec{P},\tau) \tag{1}$$

In Equation (1), the components of heat flow are denoted by q_i, the thermal conductivity is represented by symbol K, and the thermodynamic temperature is $\Theta = T - T_0$, where T_0 is the base temperature of the environment. Moreover, τ stands for the time and $\vec{P}$ is the position vector.

In the presence of an internal heat source, the principle of local energy conservation is represented as [42]:

$$\frac{\partial}{\partial\tau}[\rho C_E\Theta + \gamma_m T_0 U_{i,i}] = -q_{i,i} + S. \tag{2}$$

where the density of medium is symbolized by ρ, the elements of displacement vector are denoted by U_i, C_E is the heat capacity and S is the power of heat source.

It is assumed throughout this work that the parameters ρ, γ_m, C_E μ_0 and λ_0 are positive constants. From a purely mechanical and thermal perspectives, these are the most reasonable assumptions in this theory.

Tzou [35–37] presented a novel model representing delays in heat transfer, which incorporates two-phase-lags (t_q and t_θ) where t_q is heat flux and t_θ stands for the gradient of temperature. The following formulation of Fourier's law will then be applied in the two phase-lag model [35]:

$$q_i(\vec{P},\tau + t_q) = -K\Theta_{,i}(\vec{P},\tau + t_\theta),\ t_q > 0,\ t_\theta > 0. \tag{3}$$

The parameter t_q emphasizes the rapid transient nature of thermal effects, while parameter t_θ confirms the subtle structural processes that occur during the process. With appropriate initial and boundary conditions, it has been demonstrated by Quintanilla and Racke [43] that the system is exponentially stable when $0 < t_q < 2t_\theta$, and shows unstable behavior when $0 < 2t_\theta < t_q$.

By utilizing Taylor's series expansions for t_q and t_θ, and retaining the specific terms that depend on the nature and characteristics of material, the following equation can be obtained [39,40]:

$$\left(1 + \sum_{k=1}^{m} \frac{t_q^k}{k!}\frac{\partial^k}{\partial\tau^k}\right) q_i = -K\left(1 + \sum_{k=1}^{n} \frac{t_\theta^k}{k!}\frac{\partial^k}{\partial\tau^k}\right)\Theta_{,i}. \tag{4}$$

The temperature change and heat flow have been truncated to orders n and m, respectively.

Some restrictions on using the higher-orders of m and n are demonstrated by Chiriţă et al. [44–46]. For example, by considering $m, n > 5$, an unstable behavior is produced that is unable to present a genuine physical feature. In contrast, the Second Law of Thermodynamics must be addressed when the approximation orders are fewer than four.

By incorporating Equations (2) and (4) in the following way, one can derive the refined heat transfer equation that includes the higher-order time derivatives [39,40]:

$$\left(1+\sum_{k=1}^{m}\frac{t_q^k}{k!}\left(\frac{\partial^k}{\partial\tau^k}\right)\right)\left[\rho C_E\frac{\partial\Theta}{\partial t}+\gamma_m T_0\frac{\partial U_{i,i}}{\partial t}-S\right]=K\left(1+1\sum_{k=1}^{n}\frac{t_\theta^k}{k!}\left(\frac{\partial^k}{\partial\tau^k}\right)\right)\Theta_{,ii} \tag{5}$$

On the other hand, the stress tensor σ_{ij}, strain tensor e_{ij} and equation of motion are described as follows [39,40]

$$\sigma_{ij}=\mu_m\left(U_{j,i}+U_{i,j}\right)+\lambda_m e_{kk}\delta_{ij}-\gamma_m\Theta\delta_{ij}, \tag{6}$$

$$2e_{ij}=U_{j,i}+U_{i,j}, \tag{7}$$

$$\mu_m U_{i,jj}+(\lambda_m+\mu_m)U_{j,ij}+R_i=\rho\frac{\partial^2}{\partial\tau^2}(U_i)+\gamma_m\Theta_{,i}. \tag{8}$$

In Equations (6)–(8), the elements of the local stress tensor are denoted by σ_{ij}, the strain tensor is defined by e_{ij}, the components of body forces are represented by R_i, and i, j, k take the magnitudes of 1, 2, 3. By modifying the viscoelastic Kelvin–Voigt model, it is possible to produce a viscoelastic fractional order model and extend the thermoelastic theories. First-order time derivatives are replaced by fractional derivatives in the modified Kelvin–Voigt model. Given the new scenario, one has [47,48]

$$\mu_m=\mu_0+\mu_0\mu_1^\alpha D_\tau^\alpha,\ \lambda_m=\lambda_0+\lambda_0\lambda_1^\alpha D_\tau^\alpha,\ \gamma_m=\gamma_0+\gamma_0\gamma_1^\alpha D_\tau^\alpha, \tag{9}$$

where μ_0, λ_0 are elastic constants, μ_1, λ_1 and γ_1 are viscoelastic coefficients as follows:

$$\gamma_0=(3\lambda_0+2\mu_0)\alpha_t,\ \gamma_v=\frac{\left(3\lambda_0\lambda_1^\alpha+2\mu_0\mu_1^\alpha\right)\alpha_t}{\gamma_0}. \tag{10}$$

In the preceding relations, the concept of the Riemann–Liouville operator of order α is assumed, which can be written as follows [49–51]:

$$D_\tau^\alpha f(\tau)=\frac{1}{\Gamma(1-\alpha)}\frac{d}{dt}\int_0^\tau(\tau-\varpi)^{-\alpha}f(\varpi)\mathrm{d}\varpi,\ \alpha\in(0,1]. \tag{11}$$

The above definition can be considered as a singular kernel. The solution of such singular kernel is always challenging and in the case of fractional order has been solved by Caputo and Fabrizio [35,40,52] by introducing a new idea of the fractional derivative, which is described by the following formula:

$$CFD_\tau^\alpha f(\tau)=\frac{1}{1-\alpha}\int_0^\tau\exp\left[-\frac{\alpha}{1-\alpha}(\tau-\varpi)\right]\frac{\partial}{\partial\varpi}[f(\varpi)]\mathrm{d}\varpi,\ \alpha\in(0,1]. \tag{12}$$

In the same direction, and to deal with the non-singularity and nonlocal kernels, Atangana and Baleanu [53,54] provided a new form of fractional derivatives on the basis of Mittag–Leffler operator $E_\alpha(-t^\alpha)$.

The following formula defines the fractional operator proposed by Atangana and Baleanu [53–56]:

$$ABD_\tau^\alpha f(\tau)=\frac{1}{1-\alpha}\int_0^\tau E_\alpha\left[-\frac{\alpha(\tau-\varpi)^\alpha}{1-\alpha}\right]\frac{\partial}{\partial\varpi}[f(\varpi)]\mathrm{d}\varpi,\ \alpha\in(0,1]. \tag{13}$$

For $s > 0$, the above differential operator can be transferred into Laplace domain as [53,54]:

$$\Im[AABD_{\tau}^{\alpha} f(\tau)] = \frac{1}{s^{\alpha}(1-\alpha)+\alpha}\left[s^{\alpha}\Im[f(\tau)] - s^{\alpha-1}f(0)\right]. \tag{14}$$

According to Eringen and Edelen [16,49], the stress tensor T_{ij} at each point $\vec{P}$ of a body can be written as:

$$T_{ij}(\vec{P}) = \int_{V} \beth(|\vec{P} - \vec{P\prime}|, \chi)\sigma_{ij}(\vec{P\prime})\mathrm{d}V(\vec{P\prime}), \tag{15}$$

where $\sigma_{ij}(\vec{P\prime})$ represents the local stress tensor described by

$$\sigma_{ij}(\vec{P\prime}) = 2\mu e_{ij}(\vec{P\prime}) + \lambda\delta_{ij}e_{kk}(\vec{P\prime}) - \gamma\delta_{ij}\Theta(\vec{P\prime}). \tag{16}$$

According to Equation (15), the nonlocal stress T_{ij} at a given location $(\vec{P})$ is equal to a weighted average of classical local stresses of all locations near $\vec{P}$, where the weights are proportional to the size of nonlocal kernel $\beth(|\vec{P} - \vec{P\prime}|, \chi)$ where $|\vec{P} - \vec{P\prime}|$ is the Euclidean distance. Utilizing a calibrating constant e_0 that varies with the type of material, $\chi = e_0 a/l$ represents the proportion between the internal characteristic length a and the external characteristic length l. For instance, the following kernel can be selected [54]:

$$\beth(|\vec{P} - \vec{P\prime}|, \chi) = \frac{1}{2\pi\chi^2 l^2} K_0\left(\frac{1}{\xi l}|\vec{P} - \vec{P\prime}|\right), \tag{17}$$

in which function K_0 denotes zero-order modified Bessel functions of the second kind. For a given class of physically permissible kernel $\beth(|\vec{P} - \vec{P\prime}|, \chi)$, the integral constitutive equation given by (15) can be expressed in an alternative differential form as [16]:

$$T_{ij}(\vec{P}) - \chi^2\nabla^2 T_{ij}(\vec{P}) = \sigma_{ij}(\vec{P\prime}). \tag{18}$$

Introducing Equation (18) into Equations (6) and (8), then one has

$$T_{ij} - \chi^2\nabla^2 T_{ij} = 2\mu_m e_{ij} + \lambda_m\delta_{ij}e_{kk} - \gamma_m\delta_{ij}\Theta\,, \tag{19}$$

$$\mu_m U_{i,jj} + (\lambda_m + \mu_m)U_{j,ij} + R_i = \gamma_m\Theta_{,i} + \rho\left(\frac{\partial^2 U_i}{\partial\tau^2} - \chi^2\nabla^2\frac{\partial^2 U_i}{\partial\tau^2}\right). \tag{20}$$

The concept of inertia, defined as the tendency of a body to preserve its prior state, is not limited to mechanics; the heat capacity of bodies also delays the rate at which their thermal states change. As a result of this phenomenon, synaptic diffusion has important physical implications: it conveys the fact that if time moves faster in any sector of space, diffusion will also move faster in these places. This is where the concept of "thermal inertia" was first developed. Similar to thermal conductivity, inertia can be thought as a measure of "thermal mass" and the rate at which heat waves travel through a material. Therefore, the term of thermal mass is interchangeably used with inertia.

3. Statement of the Problem

As shown in Figure 1, in this section, the examination of viscoelastic media that is homogeneous, isotropic, and assumed as a semi-infinite body, is considered. The half-space occupies the region $X \geq 0$, where its initial temperature is equal to T_0. It is also assumed that the half-space is subjected to a periodic heat source which spreads over the boundary $X = 0$. For this probe, Cartesian coordinates (X, Y, Z) are used in which X axis is perpendicular to the free surface of the half-space. It is also supposed that the temperature as well as heat waves change in X direction.

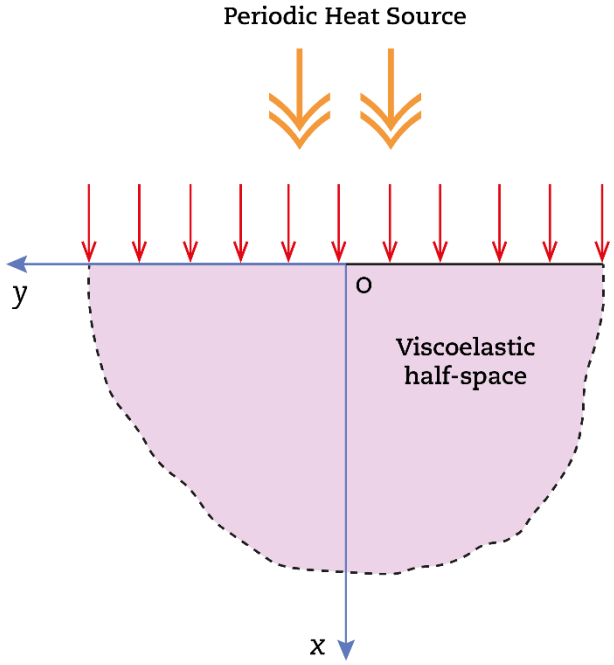

Figure 1. Schematic representation of a viscoelastic half-space in the presence of cyclic heat source.

The considered problem is simplified to a 1D problem where the only non-vanishing component of displacement vector is $U_X = U(X, \tau)$. As a consequence, the nonlocal stress T_{XX}, defined by Equation (19), may be expressed as:

$$T_{XX} - \chi^2 \frac{\partial^2 T_{XX}}{\partial X^2} = (\lambda_0 + 2\mu_0 + (\lambda_0 \lambda_1^\alpha + 2\mu_0 \mu_1^\alpha) D_\tau^\alpha) \frac{\partial U}{\partial X} - \gamma_0 (1 + \gamma_1^\alpha D_\tau^\alpha)\Theta \tag{21}$$

A unidirectional magnetic field $\vec{H} = (0, H_X, 0)$ is applied throughout the material. Maxwell's equations are used to analyze the influence of magnetic environment on the thermally conductive solid. These equations can be written in the following forms

$$\vec{J} = \sigma_e \left(\vec{E} + \mu_0 \left(\frac{\partial \vec{U}}{\partial t} \times \vec{B} \right) \right), \vec{h} = \nabla \times (\vec{U} \times \vec{H}), \vec{B} = \mu_0 \vec{H}, \nabla \cdot \vec{B} = 0 \tag{22}$$

where the induced magnetic field is characterized by the $\vec{h}$, the electric field is indicated by $\vec{E}$, the current density is $\vec{J}$, and the initial magnetic field is represented by $\vec{H}$. Moreover, the electrical conductivity and magnetic permeability are denoted by μ_e and σ_e, respectively.

Assuming that the effects of electric field are negligible and then by considering the Ohm's Law, one has [57–61]:

$$\vec{F} = -\left(\sigma_e \mu_e^2 H_X^2 \frac{\partial U}{\partial \tau}, 0, 0 \right). \tag{23}$$

Thereby, the equation of motion can be expressed as follows:

$$\begin{aligned} &\left(\tfrac{\lambda_0 + 2\mu_0}{\rho} + \tfrac{(\lambda_0 \lambda_1^\alpha + 2\mu_0 \mu_1^\alpha)}{\rho} D_\tau^\alpha \right) \tfrac{\partial^2 U}{\partial X^2} - \tfrac{\sigma_e \mu_e^2 H_X^2}{\rho} \left(\tfrac{\partial U}{\partial \tau} - \chi^2 \tfrac{\partial^3 U}{\partial \tau \partial X^2} \right) \\ &= \tfrac{\gamma_0 (1 + \gamma_1^\alpha D_\tau^\alpha)}{\rho} \tfrac{\partial \Theta}{\partial X} + \left(\tfrac{\partial^2 U}{\partial \tau^2} - \chi^2 \tfrac{\partial^2}{\partial X^2} \left(\tfrac{\partial^2 U}{\partial \tau^2} \right) \right). \end{aligned} \tag{24}$$

In addition, the extended DPL heat transfer equation, which is described by Equation (5) and includes higher-order temporal derivatives, may be written as:

$$\left(1+\sum_{k=1}^{m}\frac{t_q^k}{k!}\frac{\partial^k}{\partial\tau^k}\right)\left[\frac{\rho C_E}{K}\frac{\partial\Theta}{\partial\tau}+\frac{\gamma_0 T_0(1+\gamma_v^\alpha D_t^\alpha)}{K}\frac{\partial}{\partial\tau}\left(\frac{\partial U}{\partial X}\right)-\frac{S}{K}\right]=\frac{\partial^2\Theta}{\partial X^2}+\sum_{k=1}^{n}\frac{t_\theta^k}{k!}\frac{\partial^k}{\partial\tau^k}\left(\frac{\partial^2\Theta}{\partial X^2}\right). \tag{25}$$

In our analysis, the following nondimensional quantities will be considered:

$$\begin{array}{l}\{x,u\}=c_0\eta_0\{X,U\},\{t,\tau_q,\tau_\theta,\lambda_v,\mu_v,\gamma_v\}=c_0^2\eta_0\{\tau,t_q,t_\theta,\lambda_1,\mu_1,\gamma_1\},\\ \xi=c_0^2\eta_0^2\chi,\ \theta=\frac{\Theta}{T_0},\ \tau_{xx}=\frac{T_{XX}}{\mu_0},\ Q=\frac{S}{KT_0c_0^2\eta_0^2},\ c_0=\frac{(\lambda_0+2\mu_0)}{\rho},\eta_0=\frac{\rho C_E}{K}.\end{array} \tag{26}$$

By substituting the above quantities into Equations (21), (24), and (25), the nondimensional forms of governing equations can be simplified as:

$$\tau_{xx}-\xi^2\frac{\partial^2\tau_{xx}}{\partial x^2}=(\beta_1+\beta_2D_t^\alpha)\frac{\partial u}{\partial x}-b(1+\gamma_v^\alpha D_t^\alpha)\theta, \tag{27}$$

$$\frac{\partial^2u}{\partial t^2}-\xi^2\frac{\partial^2}{\partial x^2}\left(\frac{\partial^2u}{\partial t^2}\right)+\varepsilon\left(\frac{\partial u}{\partial t}-\xi^2\frac{\partial^2}{\partial x^2}\left(\frac{\partial u}{\partial t}\right)\right)=(\beta_1+\beta_2D_t^\alpha)\frac{\partial^2u}{\partial x^2}-b(1+\gamma_v^\alpha D_t^\alpha)\frac{\partial\theta}{\partial x}, \tag{28}$$

$$\begin{array}{c}\frac{\partial^2\theta}{\partial x^2}+\sum\limits_{k=1}^{n}\frac{\tau_\theta^k}{k!}\frac{\partial^k}{\partial t^k}\left(\frac{\partial^2\theta}{\partial x^2}\right)=\left(1+\sum\limits_{k=1}^{m}\frac{\tau_q^k}{k!}\frac{\partial^k}{\partial t^k}\right)\left[\frac{\partial\theta}{\partial t}+g(1+\gamma_v^\alpha D_t^\alpha)\frac{\partial^2u}{\partial t\partial x}\right]\\ -\left(1+\sum\limits_{k=1}^{m}\frac{\tau_q^k}{k!}\frac{\partial^kQ}{\partial t^k}\right),\end{array} \tag{29}$$

where

$$\{\beta_1,\beta_2,b\}=\frac{1}{\mu_0}\{\lambda_0+2\mu_0,\lambda_0\lambda_v^\alpha+2\mu_0\mu_v^\alpha,\gamma_0T_0\},\ \varepsilon=\frac{\sigma_e\mu_e}{c_0^2\eta_0}\left(\frac{\mu_eH_x^2}{\rho}\right),g=\gamma_0/\ \rho C_E. \tag{30}$$

For this problem, at $t=0$, the following initial requirements are imposed:

$$\theta=0=\frac{\partial^{k-1}\theta}{\partial t^{p-1}},\ u=0=\frac{\partial^{k-1}u}{\partial t^{p-1}},\ k,p=2,3,\ldots.m \text{ or } n. \tag{31}$$

It is considered that the free edge, i.e., $x=0$, is subjected to a time-varying heat supply of periodic pattern and constant strength Q_0. Consequently, the following shape for the nondimensional heat source can be postulated:

$$Q=\begin{cases}Q_0\delta(x)\sin(\pi t/t_0), & t\in[0,t_0]\\ 0, & t>t_0\end{cases}, \tag{32}$$

where the parameter t_0 is fixed, and the function $\delta(x)$ represents the well-known Dirac delta operator.

The Analytical Solution in the Laplace's Domain

The Laplace transform is an effective method for dealing with differential equations systems in engineering, physics, and other scientific disciplines. However, using the Laplace transform may result in the kind of solutions in the Laplace domain that are difficult to reverse to the time domain using the usual analytical methods. Therefore, we resort to approximate numerical solutions by using well-known algorithms in this context. The following formula characterizes the Laplace transform:

$$\overline{H}(x,t)=\int_0^\infty H(x,t)\exp[-st]dt \tag{33}$$

The result of applying the Laplace transform specified in equation (33) on Equations (27)–(29) is as follows:

$$\overline{\tau}_{xx}=\xi^2\frac{d^2\overline{\tau}_{xx}}{dx^2}+\Omega_1\frac{d\overline{u}}{dx}-\Omega_2\overline{\theta}, \tag{34}$$

$$\frac{\mathrm{d}^2\overline{u}}{\mathrm{d}x^2} = \Omega_8\overline{u} + \Omega_9\frac{\mathrm{d}\overline{\theta}}{\mathrm{d}x}, \tag{35}$$

$$\frac{\mathrm{d}^2\overline{\theta}}{\mathrm{d}x^2} = s\Omega_4\overline{\theta} + \Omega_4\Omega_3\frac{\mathrm{d}\overline{u}}{\mathrm{d}x} - \Omega_4\Omega_5\delta(x), \tag{36}$$

where

$$\begin{gathered} f(s) = s^\alpha/(s^\alpha(1-\alpha)+\alpha),\ \Omega_1 = \beta_1 + \beta_2 f(s),\ \Omega_2 = b(1+\gamma_v^\alpha f(s)), \Omega_5 = \frac{\pi t_0 Q_0}{\pi^2 + s^2 t_0^2} \\ L_q = 1 + \sum_{k=1}^{m} \frac{s^k \tau_q^k}{k!},\ L_\theta = 1 + \sum_{k=1}^{n} \frac{s^k \tau_\theta^k}{k!}, \Omega_3 = sg(1+\gamma_v^\alpha f(s)) \\ \Omega_4 = \frac{L_q}{L_\theta},\ \Omega_6 = \Omega_1 + s^2\xi^2 + \varepsilon s\xi^2, \Omega_7 = s^2 + \varepsilon s,\ \{\Omega_8, \Omega_9\} = \frac{1}{\Omega_6}\{\Omega_7, \Omega_2\} \end{gathered} \tag{37}$$

Equations (35) and (36), when represented in the vector–matrix differential form, may be expressed as [62,63]:

$$\frac{\mathrm{d}\mathbf{Y}(x,s)}{\mathrm{d}x} = \phi(s)\mathbf{Y}(x,s) - \psi(x,s), \tag{38}$$

where

$$\begin{gathered} \mathbf{Y}(x,s) = \left(\overline{\theta}, \overline{u}, \frac{\mathrm{d}\overline{\theta}}{\mathrm{d}x}, \frac{\mathrm{d}\overline{u}}{\mathrm{d}x}\right)^{T_r}, \phi(s) = \begin{pmatrix} 0 & 0 & 1 & 0 \\ 0 & 0 & 0 & 1 \\ s\Omega_4 & 0 & 0 & \Omega_4\Omega_3 \\ 0 & \Omega_8 & \Omega_9 & 0 \end{pmatrix}, \\ \psi(x,s) = \Omega_4\Omega_5(0,\ 0, \delta(x), 0)^{T_r}. \end{gathered} \tag{39}$$

Solutions can be set in the field of Laplace transform using the eigenvalue procedure, which is discussed in detail in references [62–64]. Based on this method, the solutions of functions $\overline{u}(x)$ and $\overline{\theta}(x)$ take the following forms

$$\overline{u}(x) = \frac{\Omega_9 \mathrm{e}^{-k_2 x}}{2\left(k_1^2 - k_2^2\right)} - \frac{\Omega_9 \mathrm{e}^{-k_1 x}}{2\left(k_1^2 - k_2^2\right)}, \tag{40}$$

$$\overline{\theta}(x) = \frac{\Omega_4\Omega_5 k_1\left(\Omega_8 - k_2^2\right)}{2k_1k_2\left(k_1^2 - k_2^2\right)}\mathrm{e}^{-k_2 x} - \frac{\Omega_4\Omega_5 k_2\left(\Omega_8 - k_1^2\right)}{2k_1k_2\left(k_1^2 - k_2^2\right)}\mathrm{e}^{-k_1 x}, \tag{41}$$

The parameters k_1 and k_2 satisfy the following characteristic equation of matrix $\Psi(s)$

$$k^4 - (s\Omega_4 + \Omega_8 + \Omega_9\Omega_4\Omega_3)k^2 + s\Omega_4\Omega_8 = 0, \tag{42}$$

By making the appropriate substitutions in Equation (34) using Equations (40) and (41), one can get the nonlocal stress component $\overline{\tau}_{xx}$ as follows

$$\begin{gathered} \overline{\tau}_{xx}(x) = \frac{\Omega_1\Omega_9}{2\left(k_1^2 - k_2^2\right)\left(1 - \xi^2 k_2^2\right)}\mathrm{e}^{-k_2 x} - \frac{\Omega_1\Omega_9}{2\left(k_1^2 - k_2^2\right)\left(1 - \xi^2 k_1^2\right)}\mathrm{e}^{-k_1 x} + \\ \frac{k_1\Omega_2\Omega_4\Omega_5\left(\Omega_8 - k_2^2\right)}{2k_1k_2\left(k_1^2 - k_2^2\right)\left(1 - \xi^2 k_2^2\right)}\mathrm{e}^{-k_2 x} - \frac{k_2\Omega_2\Omega_4\Omega_5\left(\Omega_8 - k_1^2\right)}{2k_1k_2\left(k_1^2 - k_2^2\right)\left(1 - \xi^2 k_1^2\right)}\mathrm{e}^{-k_1 x} \end{gathered} \tag{43}$$

4. Inversion Technique

It is sometimes difficult to obtain the analytical inversion of the obtained solutions within the Laplace transform, and therefore one has to use the numerical inversion algorithms. The Laplace inversion can be set numerically utilizing a variety of approximation algorithms available in the literature. Each method has its benefits and may be suited for a particular situation. A well-known strategy in thermoelasticity is the Zakian approximation technique which estimates the physical fields in the real-time domain [65–67]. Any function $H(x,t)$ can be approximated by Zakian method using the following relationship:

$$H(x,t) = L^{-1}[H(x,s)] = \frac{2}{t}\sum_{i=1}^{N} \mathrm{Re}\left\{Y_i \overline{H}\left(x, \frac{\alpha_i}{t}\right)\right\}. \tag{44}$$

From Equation (44), we may deduce that this strategy is simple and straightforward to apply. The factors Y_i and α_i are fixed that may be either real numbers or complex conjugate pairs. It is possible to optimize and choose appropriate N, the number of statements to be considered under the model. The values of Y_i and α_i for $N = 5$ are presented in Table 1.

Table 1. The values of Y_i and α_i in Zakian's algorithm [67].

j	α_i	Y_i
1	$12.83767675 + i666063445$	$-36902.08210 + i196990.4257$
2	$2\ 12.22613209 + i5.012718792$	$61277.02524 - i95408.62551$
3	$3\ 10.93430308 + i8.409673116$	$-28916.56288 + i18169.18531$
4	$4\ 8.776434715 + i11.92185389$	$4655.361138 - i1.901528642$
5	$5\ 5.225453361 + i15.72952905$	$-118.7414011 - i141.3036911$

5. Special Cases

The governing equation derived in this study can be converted to previous thermoelastic models that can be summarized by the following special cases:

5.1. Thermoelastic Models

When the small-scale and viscoelastic effects are ignored ($\xi = 0$ and $\mu_v = \lambda_v = 0$) one can obtain: the conventional thermoelasticity (CTE) when $\tau_q = \tau_\theta = 0$; the generalized thermoelastic theory with single phase delay (LS) if $\tau_q > 0$, $\tau_\theta = 0$ and $m = 1$; the thermoelastic dual-phase-lag system (DPL) by setting $m = n = 1$ and $\tau_q, \tau_\theta > 0$; the higher-order thermoelastic models including one phase delay (HLS) when $\tau_\theta = 0$, $\tau_q > 0$ and $m \geq 1$; and the higher-order thermoelastic model with two-phase-lags (HDPL) if $\tau_q, \tau_\theta > 0$, m, $n \geq 1$;

5.2. Thermoviscoelastic Models

When the classical Kelvin–Voigt viscoelastic model is applied ($\mu_v, \lambda_v > 0$ and $\alpha = 1$) and small-scale effects are ignored ($\xi = 0$), one gets: the conventional thermoviscoelastic (VCTE) model when $\tau_q = \tau_\theta = 0$; the generalized thermoviscoelastic theory with single phase delay (VLS) if $\tau_q > 0$, $\tau_\theta = 0$ and $m = 1$; the thermoviscoelastic dual-phase-lag theory (VDPL) by setting $m = n = 1$ and $\tau_q, \tau_\theta > 0$; the higher-order thermoviscoelastic framework with a single-phase-lag (HVLS) when $\tau_\theta = 0$, $\tau_q > 0$ and $m \geq 1$; and the higher-order thermoviscoelastic model with two-phase delays (HVDPL) if $\tau_q, \tau_\theta > 0$, m, $n \geq 1$.

5.3. Fractional Thermoviscoelastic Models

In the case of the fractional Kelvin–Voigt viscoelastic type (i.e., $\mu_v, \lambda_v > 0$ and $\alpha \in (0, 1]$) and by ignoring the small-scale effects ($\xi = 0$), one gets: the fractional conventional thermoviscoelastic theory (FVCTE) when $\tau_q = \tau_\theta = 0$; the generalized fractional thermoviscoelastic theory with single-phase-lag (FVLS) if $\tau_q > 0$, $\tau_\theta = 0$ and $m = 1$; the fractional thermoviscoelastic dual-phase-lag model (FVDPL) by setting $m = n = 1$ and $\tau_q, \tau_\theta > 0$; the fractional higher-order thermoviscoelastic model with single phase delay (FHVLS) when $\tau_\theta = 0$, $\tau_q > 0$ and $m \geq 1$; and the fractional higher-order thermoviscoelastic model with two-phase delays (FHVDPL) if $\tau_q, \tau_\theta > 0$, m, $n \geq 1$.

5.4. Nonlocal Fractional Thermoviscoelastic Models:

Finally, when the impacts of the size-dependent parameter (the nonlocal parameter) and the fractional operator are taken into account ($\xi > 0$ and $\alpha \in (0, 1]$), one can conclude: the nonlocal fractional conventional thermoviscoelastic theory (NFVCTE) when $\tau_q = \tau_\theta = 0$; the generalized nonlocal fractional thermoviscoelastic theory with single-phase-lag (NFVLS) if $\tau_q > 0$, $\tau_\theta = 0$ and $m = 1$; the nonlocal fractional thermoviscoelastic dual-phase-lag model (NFVDPL) by setting $m = n = 1$ and $\tau_q, \tau_\theta > 0$; the nonlocal fractional higher-order thermoviscoelastic framework with one-phase-lag (NFHVLS) when $\tau_\theta = 0$,

$\tau_q > 0$ and $m \geq 1$; and the nonlocal fractional higher-order thermoviscoelastic model with two-phase-lags (NFHVDPL) if $\tau_q, \tau_\theta > 0,\ m,\ n \geq 1$.

6. Results and Discussion

To examine the integrity of the proposed model in this research, some discussions on the numerical results of the studied field variables are presented. Moreover, to perform the numerical computations, the following physical values for copper material are introduced:

$$E = 128(\text{GPa}),\ \rho = 8954\left(\text{Kg/m}^3\right),\ \nu = 0.36,\ T_0 = 293\text{K}$$
$$\alpha_t = 1.78 \times 10^{-5}\left(\tfrac{1}{K}\right), K = 386\ \left(\tfrac{\text{W}}{\text{mK}}\right),\ \sigma_0 = 10^{-9}/36\pi\ (\text{F/m}),$$
$$H_{\text{x}} = \tfrac{10^{-7}}{4\pi}\left(\tfrac{\text{A}}{\text{m}}\right), \mu_0 = 4\pi \times 10^{-7}\ \left(\tfrac{\text{H}}{\text{m}}\right), C_E = 384.56\ (\text{J/kgK})$$

Although the nonlocal theorem is frequently used in many nanoscale applications, the method for calibrating the nonlocal scale parameter remains challenging; nevertheless, some predictions were already presented in the literature [68]. Using the dimensionless form of governing equation, the nonlocal parameter is estimated as, 0.1, 0.11, 0.12, and 0.13, considering that all of them are smaller than 2.0 nm in their dimensional form.

To deal with the problem, the following cases are taken into consideration:

- Comparing the thermoelastic properties of a material by considering the impact of higher-order parameters m and n.
- Comparing different thermoviscoelastic models including the fractional order derivatives.
- Comparing the classical and nonlocal thermoviscoelastic models.

6.1. Verification of the Results

The formulations proposed in this study are validated against the reported results by investigating the thermoelastic interactions in an infinite medium based on thermoelastic theory [68–70]. The differences between the numerical results reported in [25] and the present results are due to the presence of a viscoelastic model as well as the higher-order time derivatives. After comparing our findings with those presented in the literature [68–70], it is concluded that the behavior of thermomechanical waves are in good agreement with previous findings. The existence of viscoelastic coefficients, together with the higher-order derivatives, slows the internal propagation of heat waves, which is one of the main discrepancies between the results.

6.2. The Influence of Time Derivatives of Higher-orders

In the first scenario, the influence of partial derivatives of higher-orders on the interactions of different domains within the medium is analyzed. Tables 2–4 show the numerical values of domain variables versus distance x for different values of the higher-order terms m and n. For this purpose, the fractional viscoelastic Kelvin–Voigt type is used to evaluate various nonlocal thermoelastic theories. These models include the nonlocal fractional conventional thermoviscoelastic theory (NFCVTE), the fractional nonlocal thermoviscoelastic framework with single-phase-lag (NFVLS), the fractional nonlocal thermoviscoelastic system with two-phase delays (NFVDPL), and the nonlocal fractional thermoviscoelastic hypothesis with phase delays and time derivatives of higher-orders (NHFVDPL). In the numerical calculations, it is assumed that $\tau_q = 0.05$, $\tau_\theta = 0.03$, $\xi = 0.1$, $\mu_v = 0.06$, $\lambda_v = 0.09$ and $\alpha = 0.8$.

Table 2 presents the variation of temperature θ for different thermoelastic frameworks (NFCVTE, NFVLS, NFVDPL, and NHFVDPL) versus distance x. Table 2 reveals that non-zero temperatures are only found in a small area close to the surface. This is due to the fact that the heat flow is slow near the boundaries of the medium. It has also been observed that the temperature change decreases when time moves forward. The surface of the heat source has the highest temperature of the body. The temperature of the medium decays as we move away from the half-space boundaries. In addition, the higher values of temperature distribution θ can be obtained using NFCVTE theory. Higher-order terms

m and n have a prominent role in predicting the nondimensional temperature changes θ, especially for those points sufficiently close to the surface of the medium that are directly influenced by the applied heat source. Table 2 also displays that as the orders m and n increase, the temperature change decays.

Table 2. The effect of the higher-orders m and n on the variation of temperature θ.

x	NFCVTE	NFVLS	NFVDPL	NHFVDPL			
				$m = 2, n = 1$	$m = 3, n = 2$	$m = 4, n = 3$	$m = 5, n = 2$
0.0	0.0844468	0.0784302	0.0740956	0.0779163	0.0778836	0.0778821	0.077882
0.2	0.0198698	0.0204628	0.0208263	0.020509	0.0205119	0.020512	0.020512
0.4	0.00479804	0.00545069	0.00595733	0.00550921	0.00551295	0.00551313	0.00551313
0.6	0.00124161	0.00152758	0.00177424	0.00155494	0.0015567	0.00155678	0.00155678
0.8	0.000375976	0.000478265	0.000575092	0.000488623	0.000489292	0.000489323	0.000489325
1.0	0.000147462	0.000181334	0.000216234	0.000184943	0.000185178	0.000185189	0.000185189
1.2	7.54928×10^{-5}	8.65688×10^{-5}	9.88161×10^{-5}	8.77989×10^{-5}	0.000087879	8.78828×10^{-5}	8.78829×10^{-5}
1.4	0.000045809	4.96237×10^{-5}	5.40217×10^{-5}	5.00569×10^{-5}	5.00852×10^{-5}	5.00865×10^{-5}	5.00866×10^{-5}
1.6	3.00219×10^{-5}	3.15135×10^{-5}	3.32245×10^{-5}	3.16817×10^{-5}	3.16927×10^{-5}	3.16932×10^{-5}	3.16932×10^{-5}
1.8	2.02587×10^{-5}	2.09575×10^{-5}	2.17188×10^{-5}	2.10336×10^{-5}	2.10386×10^{-5}	2.10388×10^{-5}	2.10388×10^{-5}
2.0	1.38121×10^{-5}	1.42001×10^{-5}	1.45952×10^{-5}	1.42407×10^{-5}	1.42433×10^{-5}	1.42434×10^{-5}	1.42434×10^{-5}

Table 3. The influence of orders m and n on the variation of displacement u.

x	NFCVTE	NFVLS	NFVDPL	NHFVDPL			
				m =2, $n = 1$	$m = 3, n = 2$	$m = 4, n = 3$	$m = 5, n = 2$
0.0	0	0	0	0	0	0	0
0.2	−0.0295324	−0.0329637	−0.035788	−0.033282	−0.0333024	−0.0333034	−0.0333034
0.4	−0.0231758	−0.0266085	−0.0295354	−0.0269338	−0.0269547	−0.0269557	−0.0269558
0.6	−0.0152206	−0.0177062	−0.0198766	−0.0179452	−0.0179606	−0.0179613	−0.0179613
0.8	−0.00961635	−0.0112476	−0.0126914	−0.0114056	−0.0114158	−0.0114163	−0.0114163
1.0	−0.00601749	−0.00705283	−0.00797554	−0.00715354	−0.00716003	−0.00716033	−0.00716034
1.2	−0.00375625	−0.00440594	−0.00498682	−0.00446925	−0.00447333	−0.00447352	−0.00447352
1.4	−0.00234325	−0.00274939	−0.00311304	−0.002789	−0.00279155	−0.00279167	−0.00279167
1.6	−0.00146154	−0.00171512	−0.00194231	−0.00173985	−0.00174145	−0.00174152	−0.00174152
1.8	−0.000911561	−0.00106982	−0.00121166	−0.00108526	−0.00108625	−0.0010863	−0.0010863
2.0	−0.000568533	−0.000667289	−0.00075582	−0.00067693	−0.000677546	−0.000677576	−0.000677577

Table 4. The influence of higher-order terms m and n on the variation of nonlocal stress τ_{xx}.

x	NFCVTE	NFVLS	NFVDPL	NHFVDPL			
				$m = 2, n = 1$	$m = 3, n = 2$	$m = 4, n = 3$	$m = 5, n = 2$
0.0	0.0887013	0.0941639	0.0985205	0.0946607	0.0946925	0.094694	0.0946941
0.2	−0.000735809	0.000590091	0.0017973	0.000721137	0.000729581	0.000729978	0.000729992
0.4	−0.00948806	−0.0102996	−0.0109006	−0.0103704	−0.0103749	−0.0103751	−0.0103751
0.6	−0.00737191	−0.0083814	−0.00922206	−0.0084758	−0.00848186	−0.00848214	−0.00848215
0.8	−0.00483203	−0.00558685	−0.00624065	−0.0056591	−0.00566374	−0.00566396	−0.00566397
1.0	−0.00305141	−0.00355059	−0.00399112	−0.00359889	−0.00360199	−0.00360214	−0.00360215
1.2	−0.00190921	−0.00222671	−0.00250938	−0.00225758	−0.00225957	−0.00225966	−0.00225966
1.4	−0.00119173	−0.00139109	−0.00156928	−0.00141052	−0.00141177	−0.00141183	−0.00141183
1.6	−0.000743429	−0.000868077	−0.000979677	−0.00088023	−0.000881016	−0.000881053	−0.000881054
1.8	−0.000463694	−0.000541523	−0.000611258	−0.00054912	−0.000549605	−0.000549628	−0.000549629
2.0	−0.000289205	−0.00033778	−0.000381319	−0.00034252	−0.000342825	−0.000342839	−0.00034284

The induced surface of half-space has a higher temperature gradient compared to the inner points of material and therefore the highest temperatures can be found around the heat source. While the maximum temperature tends toward its steady state value very quickly, the temperature distribution needs more time to stabilize. This is due to the fact

that, while the location of peak temperature travels with the heat source, the points along its path are still cooling down.

Table 3 presents the impact of higher-orders m and n on the variation of elastic deformation u. The absolute values of deflection u are shown in Table 3, where the NHVDPL model has the smallest and the NFCVTE theory has the biggest values. In addition, it is shown that the curve representing the NFHVDPL model is less steep than that of the NFVLS theory, which is itself less steep compared to the results of NFCVTE model, and so on. The NFVLS hypothesis has a single relaxation time (τ_q), whereas the NFVDPL theory has two-phase delays (τ_q and τ_θ). Therefore, the variation of displacement pattern u is significantly influenced by relaxation and phase-delay terms τ_q and τ_θ in the presence of higher-order derivatives m and n. The values of nondimensional displacements are also seen to be initially negative, followed by a quick reduction to their peak values and a slow decay to zero. It is also evident that the values of displacement u tends to quickly decrease when $n = 4$ rather than $n < 4$.

Table 4 displays the variation of nonlocal thermal stress τ_{xx} in terms of higher-order derivatives (m and n) as well as the influence of phase lags τ_q and τ_θ. It is inferred that the amounts of thermal stress τ_{xx} seems to be sensitive to the sequence of the derivatives. To a certain extent, the magnitude of thermal stress increases with higher-order values m and n. This table also reveals that the peak amplitudes of the nonlocal stress are significantly affected by phase-delay parameters τ_q and τ_θ, which indicates the phase lag periods. The nonlocal stress provided by NHFVDPL model gets the highest values, and those generated by NFCVTE theory are the smallest values. Changes emerge to be considerable, and the stress is in compressive form in the transition zone close to the surface of the viscoelastic medium where the impact of heat source is meaningful, but the variations diminish and eventually disappear with time and distance.

The results show that the higher-order terms (m and n) of the nonlocal generalized model of thermoelasticity (HNDPL) predict a limited velocity of heat waves, similar to the other modified models, which causes the present modified model to be more suitable for predicting the material's physical characteristics [38,39]. Many researchers and scientists in this subject have only considered the first and second derivatives and ignore the higher-orders of temporal derivatives [39,71]. The proposed model and the other modified theories produce comparable results, but important distinctions must always be made. Each problem requires a different selection of higher-orders (m and n) which should be verified by experimental findings. This is the main reason for presenting the numerical results in tabular form to facilitate the comparative studies. The presented numerical results confirm that choosing $m = 4$ and $n = 3$ may be suitable for the proposed HNDPL hypothesis and produce pertinent, practical and reasonable outcomes.

The theoretical calculations and discussions lead us to conclude that considering higher-order terms m and n has meaningful effects and results in distinguishing the nonlocal thermoviscoelastic theory, including the higher-order derivatives and phase lags, from earlier theories of thermoelasticity [40]. It follows that higher values for time derivatives should be considered which cannot be always ignored. Furthermore, it has been shown [72] that this effect is due to the intrinsic behavior of delayed response of heat waves in viscoelastic nanomaterials, especially when the amount of time passed during the transient process is very short or the heat flow rate is very high.

6.3. The Effect of Nonlocal Parameter

In recent years, nanomaterials and nanostructures have received great attention due to their multidisciplinary applications and their unique mechanical, thermal, and electrical properties, which open up many possibilities and horizons in modern applications. In this section, the effects of the nonlocal parameter ξ on the responses of viscoelastic solid medium are investigated. In this case, the higher-orders terms m and n, the fractional order α, the viscoelastic parameters λ_v and μ_v, and phase lags τ_q and τ_θ are supposed to be constants.

Figures 2–4 show the numerical results based on the NHFVDPL framework when $m = 3$ and $n = 2$ are selected to analyze the effects of nonlocal parameter ξ on the deformation, distribution of temperature as well as the nonlocal thermal stress. In the numerical calculations, we take $\tau_q = 0.05$, $\tau_\theta = 0.03$, $\mu_v = 0.06$, $\lambda_v = 0.09$ and $\alpha = 0.8$. In the foundational equations with $\xi = 0$, the results are for the classical models, otherwise we consider different cases where $\xi = 0.10$, 0.11, and $\xi = 0.13$ are taken into account. According to the illustrated results, it is found that the nonlocal parameter ξ has a significant influence on the behavior of all field variables. It is also revealed that, depending on the values of the nonlocal parameter ξ, the thermoelastic and mechanical waves approach their steady state solution as the distance x increases. Figure 2 also demonstrates that the non-local parameter has a minimal impact on the temperature changes. As shown, the temperature values decrease by increasing the non-local parameter, which agrees well with the results of Ref. [73]. In other words, the presence of size effects in the governing equations leads to a decrease in the temperature of material. According to Figures 3 and 4, it can be observed that by increasing the nonlocal parameter ξ, the change of displacement increases significantly while the values of nonlocal thermal stress decrease. These findings show that for a given value of the nonlocal parameter, the thermoelastic nonlocal solutions do not inevitably converge to a stiffer material that has been observed in statically indeterminate structures. In the absence of this parameter, the stiffness of the solutions increases monotonically, just as it does in isothermal problems. Therefore, in order to accurately simulate the behavior of thin structures, the nonlocality of material must be taken into account. The nonlocal impact is a crucial aspect that cannot be disregarded when calculating stress in abrupt nanoscale heating difficulties. On the other hand, the dependence of the physical fields on the nonlocal parameter is clearly observed in the components and the nature of materials [74].

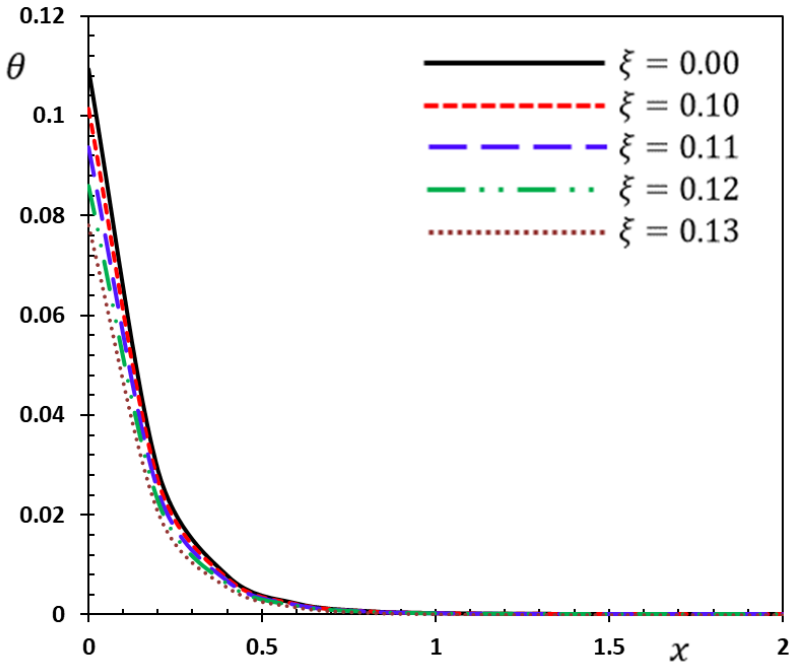

Figure 2. The variation of temperature θ versus small-scale parameter ξ.

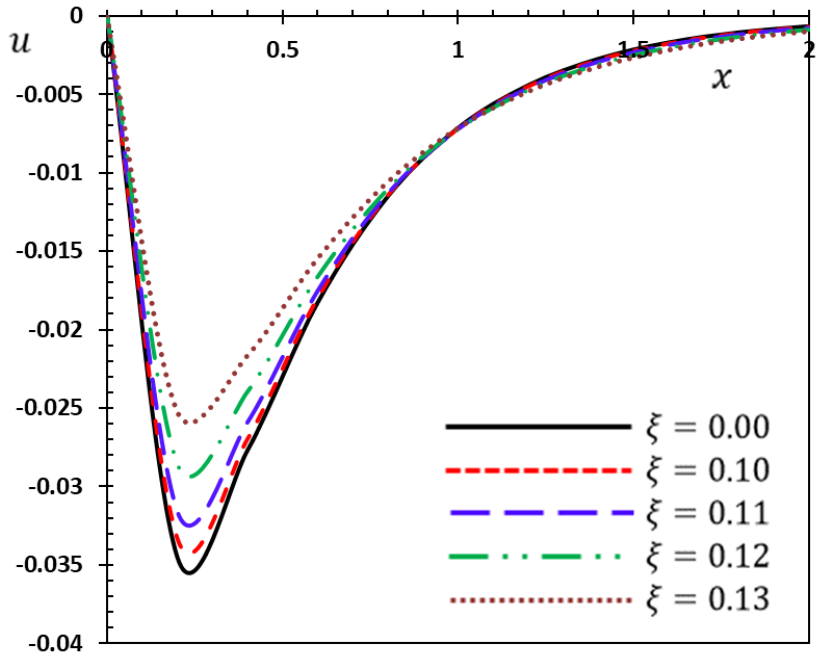

Figure 3. The variation of displacement u against the small-scale parameter ξ.

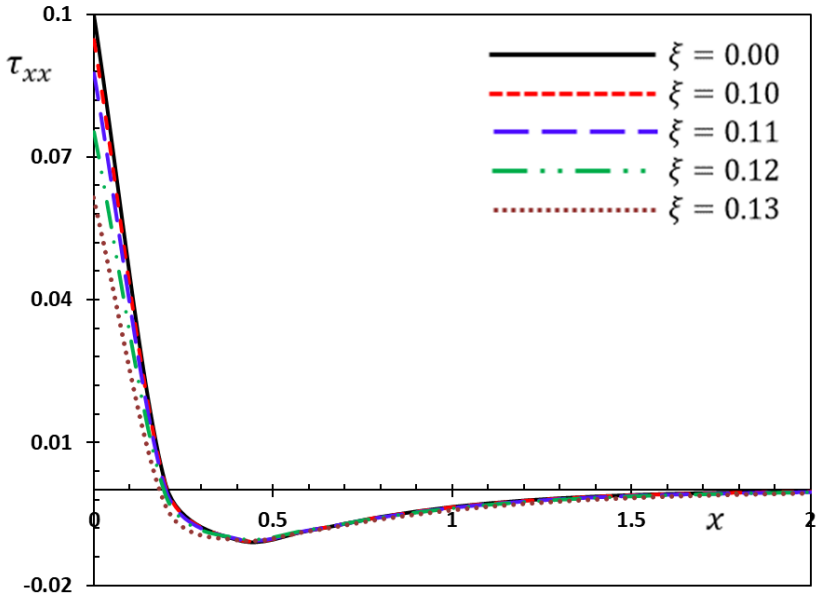

Figure 4. The variation of thermal stress τ_{xx} versus the small-scale parameter ξ.

6.4. The Influence of Viscoelasticity and Various Fractional Orders

The characteristics of viscoelastic materials are frequently time-dependent. In the models that study the behavior of viscoelastic materials, it is necessary to understand the importance of two components that represent the time-dependent viscosity, λ_v and μ_v. Other factors can be represented using these two parameters, as in described in Equations (9) and (10). Several studies have confirmed that the simplified assumptions entered into the expressions of traditional viscoelastic operators may lead to incorrect behavior of the viscoelastic media and eventually lose their physical meaning. As a result, it is physically possible to explain the transient characteristics of several elastic entities in a viscoelastic medium using Kelvin–Voigt concept, including fractional derivatives.

This article presents two methods for dealing with the fractional order heat transfer equations. The extended Mittag-Leffler function was introduced by Atangana and

Baleanu [47,48] as a novel derivative because it is better suited for describing the natural phenomena compared to the power functions. Various numerical simulations of the time-fractional heat conduction equation are generated by Atangana–Baleanu's fractional derivative operator [49,50] and the Laplace transform.

Due to the widespread application of fractional calculus in engineering and other physical fields, this article presents a viscoelastic theory of Kelvin–Voigt type that incorporates the fractional derivatives in the context of mechanical relaxation durations λ_v and μ_v. The influence of fractional orders and the viscoelastic parameters λ_v and μ_v are clarified by considering the thermoelastic theory with phase delays and higher-order time derivatives with various scenarios. The first scenario considers the nonlocal thermoelastic model with higher-order terms and phase delay (NHDPL), where the influence of viscosity is negligible ($\lambda_v = \mu_v = 0$). In the second scenario, the conventional viscoelastic model of Kelvin–Voigt type and the nonlocal thermoviscoelastic model (NHVDPL) are used ($\lambda_v, \mu_v > 0$ and $\alpha = 1$). Finally, the last case is when the assumptions of nonlocal thermoviscoelasticity (NHVDPL) are taken into consideration by employing the Kelvin–Voigt model of fractional type ($\alpha = 0.8,\ 0.6$).

The Atangana–Baleanu fractional differential operator is introduced in this study to address the issues of nonsingular and nonlocal kernels that emerge in some traditional models. It provides the basis for theoretical calculations in the case of fractional concepts ($\alpha \in (0, 1]$). In the numerical computations, we take into account the values $\tau_q = 0.05$, $\tau_\theta = 0.03$, $\mu_v = 0.06$, $\lambda_v = 0.09$ and $\xi = 0.1$. The responses of physical fields alter as a function of distance x in the presence and absence of fractional differentials as well as by considering the impact of viscoelasticity. Various comparisons are presented in Tables 5–7.

Table 5. The distribution of temperature θ for different thermoviscoelastic models.

x	Thermoelasticity	Thermo-Viscoelasticity	Fractional Thermoviscoelasticity		
	$\lambda_v = 0 = \mu_v$	$\lambda_v, \mu_v > 0$, $\alpha = 1.0$	$\lambda_v, \mu_v > 0$, $\alpha = 0.8$	$\lambda_v, \mu_v > 0$, $\alpha = 0.6$	$\lambda_v, \mu_v > 0$, $\alpha = 0.4$
0.0	0.0781856	0.077936	0.0780195	0.0780846	0.0781426
0.2	0.0206431	0.0205212	0.0205463	0.0205781	0.0206058
0.4	0.0055038	0.00549451	0.00547669	0.00547944	0.00548102
0.6	0.00150279	0.00153666	0.00151044	0.00150223	0.00149423
0.8	0.000433526	0.00047608	0.000455001	0.000444614	0.000434965
1.0	0.000139912	0.000178855	0.000165263	0.000155729	0.000147098
1.2	5.41505×10^{-5}	8.63547×10^{-5}	7.89724×10^{-5}	7.10159×10^{-5}	6.39757×10^{-5}
1.4	2.58301×10^{-5}	5.13507×10^{-5}	4.82947×10^{-5}	4.18825×10^{-5}	3.63333×10^{-5}
1.6	1.45214×10^{-5}	3.43223×10^{-5}	3.40053×10^{-5}	0.000028907	2.45912×10^{-5}
1.8	8.97000×10^{-6}	2.41463×10^{-5}	2.54236×10^{-5}	0.000021392	1.80528×10^{-5}
2.0	5.79000×10^{-6}	1.73287×10^{-5}	1.94329×10^{-5}	1.62522×10^{-5}	1.36739×10^{-5}

It is clear that the distributions of different field variables have similar trends with different values and wave propagation speeds. According to the reported numerical results, there are major discrepancies between the standard deviations of conventional thermoviscoelastic theories and those of the modified thermoviscoelastic models with fractional orders [47,48]. Unlike the traditional viscoelastic models, the fractional Atangana–Baleanu model allows for greater flexibility as indicated in Tables 5–7, which depict the physical interactions related to the transmission of thermo-mechanical vibrations [55].

As shown in Table 4, the influence of fractional derivatives on the distribution of temperature field is minimal. Tables 5–7 reveal that the viscoelastic parameters λ_v and μ_v of Kelvin–Voigt model significantly affects the variations of all physical fields under investigation. Because of their visco-thermoelastic properties, thermoelastic materials have a lower rate of heat and mechanical waves within the body. The fractional order values allow to deal with the viscoelastic materials using Kelvin–Voigt type model. Since heat

transfer is directly related to how the viscoelastic material behaves, the fractional parameter becomes even more important [50,51].

Table 6. The distribution of displacement u for different thermoviscoelastic models.

x	**Thermoelasticity**	**Thermo−Viscoelasticity**	**Fractional Thermoviscoelasticity**		
	$\lambda_v = 0 = \mu_v$	$\lambda_v, \mu_v > 0$, $\alpha = 1.0$	$\lambda_v, \mu_v > 0$, $\alpha = 0.8$	$\lambda_v, \mu_v > 0$, $\alpha = 0.6$	$\alpha = 0.4$
0.0	0	0	0	0	0
0.2	−0.0280434	−0.024395	−0.0214702	−0.0199903	−0.0183262
0.4	−0.024019	−0.0194781	−0.0195899	−0.0181806	−0.0166709
0.6	−0.0170699	−0.0127567	−0.0149597	−0.0138282	−0.0126798
0.8	−0.0116206	−0.00795342	−0.0109903	−0.0101148	−0.00927362
1.0	−0.00782119	−0.00488853	−0.00799708	−0.0073269	−0.0067164
1.2	−0.00524755	−0.00299181	−0.00580481	−0.00529412	−0.00485208
1.4	−0.00351774	−0.0018286	−0.00421086	−0.00382284	−0.00350296
1.6	−0.00235758	−0.00111719	−0.0030541	−0.00275997	−0.00252854
1.8	−0.00157993	−0.000682468	−0.00221502	−0.00199253	−0.00182509
2.0	−0.00105878	−0.00041689	−0.00160645	−0.00143847	−0.00131732

Table 7. The values of stress τ_{xx} for different thermoviscoelastic models.

x	**Thermoelasticity**	**Thermo−Viscoelasticity**	**Fractional Thermoviscoelasticity**		
	$\lambda_v = 0 = \mu_v$	$\lambda_v, \mu_v > 0$, $\alpha = 1.0$	$\lambda_v, \mu_v > 0$, $\alpha = 0.8$	$\lambda_v, \mu_v > 0$, $\alpha = 0.6$	$\alpha = 0.4$
0.0	0.0943924	0.0524847	0.0276607	0.0240686	0.0222463
0.2	0.000881063	−0.00108605	−0.0203086	−0.0180733	−0.0164797
0.4	−0.0110335	−0.00688164	−0.0222848	−0.0196959	−0.0180083
0.6	−0.00956015	−0.00537017	−0.0175763	−0.0154659	−0.0141468
0.8	−0.00681027	−0.00349919	−0.0130119	−0.0113991	−0.0104267
1.0	−0.00463903	−0.00217852	−0.00948645	−0.00827316	−0.0075664
1.2	−0.00312279	−0.00133844	−0.00688932	−0.00598084	−0.00546893
1.4	−0.0020953	−0.000819026	−0.00499821	−0.00431927	−0.00394882
1.6	−0.00140462	−0.00050057	−0.00362528	−0.00311849	−0.00285047
1.8	−0.000941376	−0.000305822	−0.00262929	−0.00225137	−0.00205747
2.0	−0.000630866	−0.00018682	−0.0019069	−0.00162534	−0.00148506

By comparing the results of displacement for the traditional viscoelastic model and those from Kelvin–Voigt type with fractional derivatives (Table 6), it is clear that the latter yields smaller values. Therefore, the fractal parameter mitigates the impact of medium deformation and mechanical waves. When fractional derivatives describe the viscoelastic behavior of materials rather than the integer derivatives, it is found that there is an excellent agreement between these findings and those of experimental observations [48,56]. Furthermore, an object's history may influence its structural phenomena. Computational results demonstrate that the fractional derivative concepts is applicable for modeling the viscoelastic materials utilized in advanced machinery and tiny devices [54,55]. Near the body's surface, where the influence of the heat source is noticeable, the variation of thermal stress τ_{xx} is more localized. When the viscoelastic factors are considered, the nonlocal stress component naturally slows down as time moves forward. The results obtained in this research can be used to design a variety of heat-exposed viscoelastic components that are used to fabricate tiny structures and devices.

7. Conclusions

Based on Eringen's nonlocal elasticity theory and the recently released thermoelastic concepts with dual-phase-lag, this investigation proposed a nonlocal thermoviscoelastic framework with higher-order time derivatives. The Kelvin–Voigt viscoelastic type of fractional order was also considered based on the Atangana and Baleanu's fractional operators. The developed model can be abstracted to the other classical and nonlocal thermoviscoelastic theories. From the observed findings, the following conclusions can be drawn:

- It is necessary to consider the effect of non-local parameters to estimate the thermomechanical behavior of nanosystems.
- The selection of higher-orders may vary from case to case and some experiments must be conducted to determine the values of higher-orders terms.
- As the coefficients of higher-order derivatives increase, a specific reduction in temperature can be seen.
- The propagation of heat waves and the variation of physical variables are profoundly affected by thermoviscoelastic features of nanomaterials.
- The numerical results under the influence of models with fractional derivatives differ from those in the case of those theories including integer derivatives.
- Numerical investigations showed that the fractional derivative models may be suitable for simulating the viscoelastic materials. These results represented a significant departure from previous approaches and exhibited a transition to a new paradigm, namely the theory of nonlocal thermoviscoelasticity based on the higher-order partial differential equations.
- The nonlocal parameter may emerge as a significant criterion in categorizing particular materials when the transmission of thermal energy is of concern in miniaturized systems and devices.

Author Contributions: Writing, review and editing, A.E.A. and H.M.S. All authors have read and agreed to the published version of the manuscript.

Funding: H.M. Sedighi is grateful to the Research Council of Shahid Chamran University of Ahvaz for its financial support (Grant No. SCU.EM1401.98).

Data Availability Statement: Not applicable.

Conflicts of Interest: The authors declare no conflict of interest.

References

1. Abazari, A.M.; Safavi, S.M.; Rezazadeh, G.; Villanueva, L.G. Modelling the Size Effects on the Mechanical Properties of Micro/Nano Structures. *Sensors* **2015**, *15*, 28543–28562. [CrossRef] [PubMed]
2. Jena, S.K.; Chakraverty, S.; Malikan, M.; Mohammad-Sedighi, H. Hygro-Magnetic Vibration of the Single-Walled Carbon Nanotube with Nonlinear Temperature Distribution Based on a Modified Beam Theory and Nonlocal Strain Gradient Model. *Int. J. Appl. Mech.* **2020**, *12*, 2050054. [CrossRef]
3. Durkan, C.; Welland, M.E. Size effects in the electrical resistivity of polycrystalline nanowires. *Phys. Rev. B* **2000**, *61*, 14215–14218. [CrossRef]
4. Mengotti, E.; Heyderman, L.J.; Rodríguez, A.F.; Nolting, F.; Hügli, R.V.; Braun, H.-B. Real-space observation of emergent magnetic monopoles and associated Dirac strings in artificial kagome spin ice. *Nat. Phys.* **2011**, *7*, 68–74. [CrossRef]
5. Villanueva, L.G.; Karabalin, R.B.; Matheny, M.H.; Chi, D.; Sader, J.; Roukes, M.L. Nonlinearity in nanomechanical cantilevers. *Phys. Rev. B* **2013**, *87*, 024304. [CrossRef]
6. Ghodrati, B.; Yaghootian, A.; Zadeh, A.G.; Mohammad-Sedighi, H. Lamb wave extraction of dispersion curves in micro/nano-plates using couple stress theories. *Waves Random Complex Media* **2018**, *28*, 15–34. [CrossRef]
7. Zare, J.; Shateri, A.; Beni, Y.T.; Ahmadi, A. Vibration analysis of shell-like curved carbon nanotubes using nonlocal strain gradient theory. *Math. Methods Appl. Sci.* **2020**. [CrossRef]
8. Civalek, Ö.; Dastjerdi, S.; Akgöz, B. Buckling and free vibrations of CNT-reinforced cross-ply laminated composite plates. *Mech. Based Des. Struct. Mach.* **2020**, *50*, 1914–1931. [CrossRef]
9. Akgoz, B.; Civalek, O. Thermo-mechanical buckling behavior of functionally graded microbeams embedded in elastic medium. *Int. J. Eng. Sci.* **2014**, *85*, 90–104. [CrossRef]

10. Sae-Long, W.; Limkatanyu, S.; Sukontasukkul, P.; Damrongwiriyanupap, N.; Rungamornrat, J.; Prachasaree, W. Fourth-order strain gradient bar-substrate model with nonlocal and surface effects for the analysis of nanowires embedded in substrate media. *Facta Univ. Ser. Mech. Eng.* **2021**, *19*, 657–680. [CrossRef]
11. Civalek, Ö.; Demir, C. A simple mathematical model of microtubules surrounded by an elastic matrix by nonlocal finite element method. *Appl. Math. Comput.* **2016**, *289*, 335–352. [CrossRef]
12. Koutsoumaris, C.C.; Eptaimeros, K.G.; Tsamasphyros, G.J. A different approach to Eringen's nonlocal integral stress model with applications for beams. *Int. J. Solids Struct.* **2017**, *112*, 222–238. [CrossRef]
13. E Abouelregal, A. Thermoelastic fractional derivative model for exciting viscoelastic microbeam resting on Winkler foundation. *J. Vib. Control* **2021**, *27*, 2123–2135. [CrossRef]
14. Eringen, A.C. Nonlocal polar elastic continua. *Int. J. Eng. Sci.* **1972**, *10*, 1–16. [CrossRef]
15. Eringen, A.C. On differential equations of nonlocal elasticity and solutions of screw dislocation and surface waves. *J. Appl. Phys.* **1983**, *54*, 4703–4710. [CrossRef]
16. Eringen, A.-C.; Edelen, D.-B. On nonlocal elasticity. *Int. J. Eng. Sci.* **1972**, *10*, 233–248. [CrossRef]
17. Inan, E.; Eringen, A. Nonlocal theory of wave propagation in thermoelastic plates. *Int. J. Eng. Sci.* **1991**, *29*, 831–843. [CrossRef]
18. Sarrami-Foroushani, S.; Azhari, M. Nonlocal vibration and buckling analysis of single and multi-layered graphene sheets using finite strip method including van der Waals effects. *Phys. E Low-Dimens. Syst. Nanostructures* **2014**, *57*, 83–95. [CrossRef]
19. Lim, C.; Zhang, G.; Reddy, J. A higher-order nonlocal elasticity and strain gradient theory and its applications in wave propagation. *J. Mech. Phys. Solids* **2015**, *78*, 298–313. [CrossRef]
20. Ma, H.; Gao, X.-L.; Reddy, J. A microstructure-dependent Timoshenko beam model based on a modified couple stress theory. *J. Mech. Phys. Solids* **2008**, *56*, 3379–3391. [CrossRef]
21. Silling, S. Reformulation of elasticity theory for discontinuities and long-range forces. *J. Mech. Phys. Solids* **2000**, *48*, 175–209. [CrossRef]
22. Nawaz, Y.; Arif, M.S.; Abodayeh, K. A Third-Order Two-Stage Numerical Scheme for Fractional Stokes Problems: A Comparative Computational Study. *J. Comput. Nonlinear Dynam.* **2022**, *17*, 101004. [CrossRef]
23. Nawaz, Y.; Arif, M.S.; Abodayeh, K. An explicit-implicit numerical scheme for time fractional boundary layer flows. *Int. J. Numer. Methods Fluids* **2022**, *94*, 920–940. [CrossRef]
24. Abouelregal, A.E.; Mohammad-Sedighi, H.; Faghidian, S.A.; Shirazi, A.H. Temperature-dependent physical characteristics of the rotating nonlocal nanobeams subject to a varying heat source and a dynamic load. *Facta Univ. Ser. Mech. Eng.* **2021**, *19*, 633–656. [CrossRef]
25. Nasr, M.E.; Abouelregal, A.E.; Soleiman, A.; Khalil, K.M. Thermoelastic Vibrations of Nonlocal Nanobeams Resting on a Pasternak Foundation via DPL Model. *J. Appl. Comput. Mech.* **2021**, *7*, 34–44. [CrossRef]
26. Abouelregal, A.E.; Mohammed, W.W.; Mohammad-Sedighi, H. Vibration analysis of functionally graded microbeam under initial stress via a generalized thermoelastic model with dual-phase lags. *Arch. Appl. Mech* **2021**, *91*, 2127–2142. [CrossRef]
27. Abouelregal, A.; Ersoy, H.; Civalek, Ö. Solution of Moore–Gibson–Thompson Equation of an Unbounded Medium with a Cylindrical Hole. *Mathematics* **2021**, *9*, 1536. [CrossRef]
28. Abouelregal, A.E. Thermomagnetic behavior of a nonlocal finite elastic rod heated by a moving heat source via a fractional derivative heat equation with a non-singular kernel. *Waves Random Complex Media* **2021**, 1–21. [CrossRef]
29. Abouelregal, A.E. A novel model of nonlocal thermoelasticity with time derivatives of higher order. *Math. Methods Appl. Sci.* **2020**, *43*, 6746–6760. [CrossRef]
30. Abouelregal, A.E.; Marin, M. The Size-Dependent Thermoelastic Vibrations of Nanobeams Subjected to Harmonic Excitation and Rectified Sine Wave Heating. *Mathematics* **2020**, *8*, 1128. [CrossRef]
31. E Aboueregal, A.; Sedighi, H.M. The effect of variable properties and rotation in a visco-thermoelastic orthotropic annular cylinder under the Moore–Gibson–Thompson heat conduction model. *Proc. Inst. Mech. Eng. Part L: J. Mater. Des. Appl.* **2021**, *235*, 1004–1020. [CrossRef]
32. Fotouhi, M.; Fragassa, C.; Fotouhi, S.; Saghafi, H.; Minak, G. Damage Characterization of Nano-Interleaved CFRP under Static and Fatigue Loading. *Fibers* **2019**, *7*, 13. [CrossRef]
33. Giaglianoni, W.; Cunha, M.; Bergmann, C.; Fragassa, C.; Pavlovic, A. Synthesis, Characterization and Application by HVOF of a WCCoCr/NiCr Nanocomposite as Protective Coating Against Erosive Wear. *Tribol. Ind.* **2018**, *40*, 477–487. [CrossRef]
34. Fragassa, C.; Cristiano, F. Modelling the viscoelastic response of ceramic materials by commercial finite elements codes. *FME Trans.* **2016**, *44*, 58–64. [CrossRef]
35. Tzou, D.Y. A Unified Field Approach for Heat Conduction from Macro- to Micro-Scales. *J. Heat Transf.* **1995**, *117*, 8–16. [CrossRef]
36. Tzou, D.Y. The generalized lagging response in small-scale and high-rate heating. *Int. J. Heat Mass Transf.* **1995**, *38*, 3231–3240. [CrossRef]
37. Tzou, D.-Y. *Macro-to Microscale Heat Transfer: The Lagging Behavior*; Taylor & Francis: New York, NY, USA, 1997.
38. Abouelregal, A. On Green and Naghdi Thermoelasticity Model without Energy Dissipation with Higher Order Time Differential and Phase-Lags. *J. Appl. Comput. Mech.* **2020**, *6*, 445–456. [CrossRef]
39. Abouelregal, A. A novel generalized thermoelasticity with higher-order time-derivatives and three-phase lags. *Multidiscip. Model. Mater. Struct.* **2019**, *16*, 689–711. [CrossRef]
40. Caputo, M.; Fabrizio, M. A new definition of fractional derivative without singular kernel. *Progr. Fract. Differ. Appl.* **2015**, *1*, 73–85.

41. Fourier, J.B.J. *Analytical Theory of Heat*; Encyclopedia Britannica, Inc.: Chicago IL, USA, 1952.
42. Chandrasekharaiah, D.S. Hyperbolic Thermoelasticity: A Review of Recent Literature. *Appl. Mech. Rev.* **1998**, *51*, 705–729. [CrossRef]
43. Quintanilla, R.; Racke, R. A note on stability in dual-phase-lag heat conduction. *Int. J. Heat Mass Transf.* **2006**, *49*, 1209–1213. [CrossRef]
44. Chiriţă, S.; Ciarletta, M.; Tibullo, V. On the thermomechanical consistency of the time differential dual-phase-lag models of heat conduction. *Int. J. Heat Mass Transf.* **2017**, *114*, 277–285. [CrossRef]
45. Chiriţă, S.; Ciarletta, M.; Tibullo, V. On the wave propagation in the time differential dual-phase-lag thermoelastic model. *Proc. R. Soc. A: Math. Phys. Eng. Sci.* **2015**, *471*, 20150400. [CrossRef]
46. Chiriţă, S. High-order approximations of three-phase-lag heat conduction model: Some qualitative results. *J. Therm. Stress.* **2018**, *41*, 608–626. [CrossRef]
47. Bagley, R.L.; Torvik, P.J. Fractional calculus in the transient analysis of viscoelastically damped structures. *AIAA J.* **1985**, *23*, 918–925. [CrossRef]
48. Bagley, R. On the equivalence of the Riemann–Liouville and the Caputo fractional order derivatives in modeling of linear viscoelastic materials. *Fract. Calcul. Appl. Anal.* **2007**, *10*, 123–126.
49. Podlubny, I. *Fractional Differential Equations: An Introduction to Fractional Derivatives, Fractional Differential Equations, to Methods of Their Solution and Some of Their Applications*; Academic Press: San Diego, CA, USA, 1999.
50. Mainardi, F. *Fractional Calculus and Waves in Linear Viscoelasticity—An Introduction to Mathematical Models*; Imperial College Press: London, UK, 2010.
51. Samko, S.G.; Kilbas, A.A.; Marichev, O.I. *Fractional Integrals and Derivatives: Theory and Applications*; Taylor & Francis: London, UK, 2002.
52. Caputo, M.; Fabrizio, M. On the notion of fractional derivative and applications to the hysteresis phenomena. *Meccanica* **2017**, *52*, 3043–3052. [CrossRef]
53. Atangana, A.; Baleanu, D. New fractional derivatives with nonlocal and nonsingular kernel: Theory and application to heat transfer model. *Therm. Sci.* **2016**, *20*, 763–769. [CrossRef]
54. Atangana, A.; Baleanu, D. Caputo-Fabrizio Derivative Applied to Groundwater Flow within Confined Aquifer. *J. Eng. Mech.* **2016**, *143*, D4016005. [CrossRef]
55. Atangana, A.; Koca, I. Chaos in a simple nonlinear system with Atangana–Baleanu derivatives with fractional order. *Chaos Solitons Fractals* **2016**, *89*, 447–454. [CrossRef]
56. Frederico Gastao, S.F.; Torres Delfim, F.M. Fractional optimal control in the sense of Caputo and the fractional Noether's theorem. *Int. Math. Forum* **2008**, *3*, 1–17.
57. Ezzat, M.; Youssef, H.M. State Space Approach for Conducting Magneto-Thermoelastic Medium with Variable Electrical and Thermal Conductivity Subjected to Ramp-Type Heating. *J. Therm. Stress.* **2009**, *32*, 414–427. [CrossRef]
58. Youssef, H. Generalized magneto-thermoelasticity in a conducting medium with variable material properties. *Appl. Math. Comput.* **2006**, *173*, 822–833. [CrossRef]
59. Abbas, I.A.; Youssef, H. Finite element analysis of two-temperature generalized magneto-thermoelasticity. *Arch. Appl. Mech.* **2009**, *79*, 917–925. [CrossRef]
60. Othman, M.I.A.; Abd-Elaziz, E.M. Effect of initial stress and Hall current on a magneto-thermoelastic porous medium with microtemperatures. *Indian J. Phys.* **2019**, *93*, 475–485. [CrossRef]
61. Kaur, I.; Lata, P.; Singh, K. Effect of Hall current in transversely isotropic magneto-thermoelastic rotating medium with fractional-order generalized heat transfer due to ramp-type heat. *Indian J. Phys.* **2021**, *95*, 1165–1174. [CrossRef]
62. Bachher, M.; Sarkar, N. Nonlocal theory of thermoelastic materials with voids and fractional derivative heat transfer. *Waves Random Complex Media* **2019**, *29*, 595–613. [CrossRef]
63. Sarkar, N. On the discontinuity solution of the Lord–Shulman model in generalized thermoelasticity. *Appl. Math. Comput.* **2013**, *219*, 10245–10252. [CrossRef]
64. Abouelregal, A.E.; Mohammad-Sedighi, H.; Shirazi, A.H.; Malikan, M.; Eremeyev, V.A. Computational analysis of an infinite magneto-thermoelastic solid periodically dispersed with varying heat flow based on non-local Moore–Gibson–Thompson approach. *Contin. Mech. Thermodyn.* **2021**, *34*, 1067–1085. [CrossRef]
65. Zakian, V. Numerical inversions of Laplace transforms. *Electron. Lett.* **1969**, *327*, 120–121. [CrossRef]
66. Halsted, D.J.; Brown, D.E. Zakian's technique for inverting Laplace transform. *Chem. Eng. J.* **1972**, *3*, 312–313. [CrossRef]
67. Zakian, V. Properties of IMN approximants. In *Pade Approximants and Their Applications*; Graves-Morris, P.R., Ed.; Academic Press: London, UK, 1973.
68. Solnechnyi, E.M.; Cheremushkina, L.A. Dynamic Properties of a One-Dimensional Heat Transfer System with a Moving Heat Source. *Autom. Remote Control* **2022**, *83*, 1172–1179. [CrossRef]
69. Banik, S.; Kanoria, M. Generalized thermoelastic interaction in a functionally graded isotropic unbounded medium due to varying heat source with three-phase-lag effect. *Math. Mech. Solids* **2012**, *18*, 231–245. [CrossRef]
70. Das, A.; Das, B. One dimensional coupled thermoelastic problem due to periodic heating in a semi-infinite rod. *IOSR J. Math.* **2012**, *3*, 15–18.

71. Kostyrko, S.; Grekov, M.; Altenbach, H. Stress concentration analysis of nanosized thin-film coating with rough interface. *Contin. Mech. Thermodyn.* **2019**, *31*, 1863–1871. [CrossRef]
72. Chiriță, S. On the time differential dual-phase-lag thermoelastic model. *Meccanica* **2017**, *52*, 349–361. [CrossRef]
73. Ge, X.; Li, P.; Fang, Y.; Yang, L. Thermoelastic damping in rectangular microplate/nanoplate resonators based on modified nonlocal strain gradient theory and nonlocal heat conductive law. *J. Therm. Stress.* **2021**, *44*, 690–714. [CrossRef]
74. Kumar, R.; Miglani, A.; Rani, R. Transient analysis of nonolocal microstretch thermoelastic thick circular plate with phase lags. *Med. J. Model. Simul.* **2018**, *09*, 25–42.